JOURNAL OF OPTOELECTRONICS AND ADVANCED MATERIALS Vol. 10, No. 1, January 2008, p. 164 - 168

# Investigation of multiple pulsing and hysteresis phenomena in the erbium-doped double-clad fiber laser

A. HABOUCHA, A. KOMAROV[a], H. LEBLOND, M. SALHI, F. SANCHEZ[*]
*Laboratoire POMA, UMR CNRS 6136, Université d'Angers, 2 Bd Lavoisier, 49000 Angers, France*
*[a]Institute of Automation and Electrometry, Russian Academy of Sciences, Acad. Koptyug Pr., 1, 630090 Novosibirsk, Russia*

We investigate both experimentally and theoretically the multiple pulsing behaviour of an erbium-doped double-clad fiber laser passively mode-locked through nonlinear polarization rotation. Hysteresis phenomena are found experimentally in both the normal and anomalous dispersion regime. Theoretical results are compared with experimental data allowing to fix the range of validity of the model.

(Received November 27, 2007; accepted January 10, 2008)

*Keywords*: Double-clad fiber laser, Multiple pulsing, Hysteresis, Erbium-doped

## 1. Introduction

In addition to telecommunication applications, self-started, passively mode-locked fiber lasers are very attractive for dynamical studies because they exhibit a large variety of behaviours. Indeed, apart from the regular single-pulse mode-locking regime, many regimes involving several pulses by cavity round-trip have been observed or theoretically predicted. First experiments were obtained using the figure eight lasers. It was reported bunches of pulses, pulses randomly spaced but well separated and also harmonic mode-locking, where the pulses are equally separated along the cavity [1-5]. In the case of multiple pulsing, it was shown that the pulses disappear one by one when the pump was decreased [5]. It is now established that multiple pulsing is a general feature of mode-locked fiber lasers independently of the exact experimental configuration. This behaviour has been reported in figure eight lasers, in fiber lasers exploiting the nonlinear polarization rotation (NLPR) and also in the stretched pulse configuration [6-9]. In the case of lasers based on the NLPR, many interesting regimes involving several pulses by cavity round-trip have been identified: harmonic mode-locking, multistability versus the pump power, pulse splitting, pulse fragmentation and bound states of two or more pulses [10-12]. In fact, most of the previous operating regimes can be observed in the majority of passively mode-locked fiber lasers independently of the exact optical configuration and they can be generated by a simple rotation of an intra-cavity phase plate. Indeed, most of experimental setups include one or more intracavity phase plates allowing the optimization of the laser.

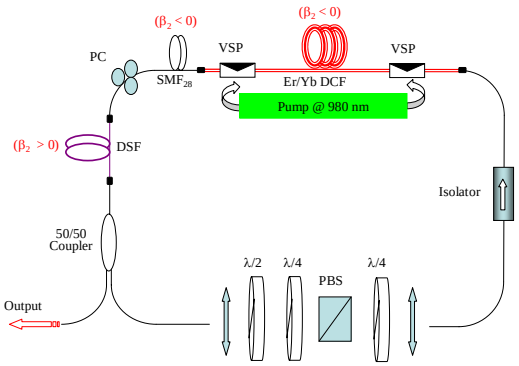


*Fig. 1. Experimental setup. PC: polarization controller, PBS: polarization beam-splitter, DSF: dispersion shifted fiber, DCF: double-clad fiber, VSP: V-groove side-pumping, SMF: standard single mode fiber at 1.5 µm.*

From the theoretical point of view, first models were based on a master equation which had the advantage to be simple, but which did not take into account the important role played by the phase plates [13,14]. They included the group velocity dispersion (GVD), the optical Kerr nonlinearity and the gain. More complex models involving two nonlinear coupled equations (one for each electric field component) have been also developed [15]. First attempt to develop a scalar model taking into account the orientation of the phase plates has been recently developed by our group [16]. It includes the GVD, the optical Kerr effect, the birefringence and linear gain (saturation effects were neglected). The resulting equation is of cubic complex Ginzburg-Landau type where the coefficients explicitly depend on the orientation angles of the phase plates. The main advantage of this model is that it leads to analytical solutions then simplifying further stability analysis, its major drawback is that it does not take into

account gain saturation thus impeding any hysteresis phenomena versus the pumping power. In a recent paper [17], we have developed a more elaborated scalar theory allowing to model multiple pulsing and multistability. Further investigation of this model showed that it could be reduced to a quintic complex Ginzburg-Landau equation where the coefficients are related to physical parameters [18].

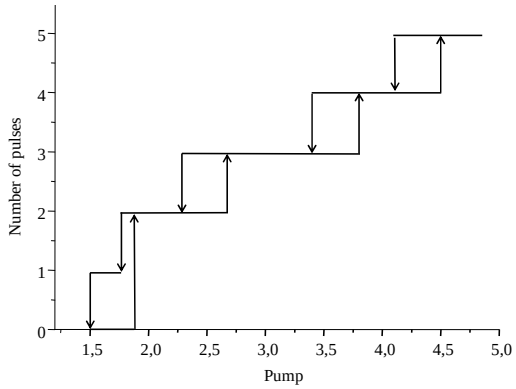


*Fig. 2. Experimental evolution of the number of pulses as a function of the pump power in the normal dispersion regime.*

Although many results have been reported on multistability in fiber lasers, none of them concerns a high-power double-clad fiber laser. The aim of this work is to investigate experimentally and theoretically multiple pulsing regimes in a passively mode-locked double-clad erbium-doped fiber laser. We first present the experimental results obtained with an erbium-doped double-clad fiber laser operating at 1.55 μm in a unidirectional ring cavity. Management of the cavity dispersion allows us to investigate both the positive and negative dispersion cases. Multiple pulsing and hysteresis phenomena are demonstrated. Section III is devoted to the theoretical part of this work. We consider the theoretical model developed for a fiber laser passively mode-locked through nonlinear polarization rotation [17]. We investigate the real case of an erbium doped fiber ring laser operating either in the normal or in the anomalous dispersion regime. In both cases, multiple pulsing is found by a suitable adjustment of the intra-cavity phase plates. A comparison with experimental data will allow to fix some limit of validity of the model.

## 2. Experiment

The experiments have been performed with an erbium-ytterbium doped double-clad fiber amplifier in a unidirectional ring cavity operating at 1.55 μm [19]. The double-clad fiber consists in a single-mode core doped with ytterbium (for the pumping) and erbium ions (emitting at 1.55μm) and two clads. The large diameter inner cladding allows having the multimode propagation of the pump beam thus allowing to use compact high power semiconductor lasers for the optical pumping. In addition, the inner cladding has a flower shape in order to break the cylindrical symmetry and then to increase the pump absorption coefficient. Two semiconductor laser diodes in counter-propagating configuration are used, both have an available output power of about 3.5 W. The V-groove technique is employed to launch the light into the fiber [19]. This technique allows to let the fiber ends free and is then well adapted for ring laser cavities. An independent-polarization optical isolator is used to obtain unidirectional oscillation. The double-clad fiber (DCF) and the standard SMF fiber have anomalous dispersion ($\beta_2 < 0$). In order to manage the total cavity dispersion, a piece of dispersion shifted fiber is used (DSF, $\beta_2 > 0$). The different lengths are such that the laser operates in the stretched pulse regime where the total cavity dispersion is slightly positive or negative. The mode-locking is achieved through nonlinear polarization rotation occurring in the fibers combined with the intracavity polarization beam splitter (the set results in a fast nonlinear absorption). Three phase plates are also used in order to change the operating regime of the laser. Indeed, a simple rotation of a phase plate allows to observe different regime such as continuous, Q-switch, regular mode-locking, multiple pulsing, etc [20]. A 50/50 single-mode fiber coupler is used to extract the energy from the cavity. The output is analysed with a 12 GHz photodetector and a 12 GHz oscilloscope. An optical spectrum analyzer and an optical autocorrelator are also used when needed.

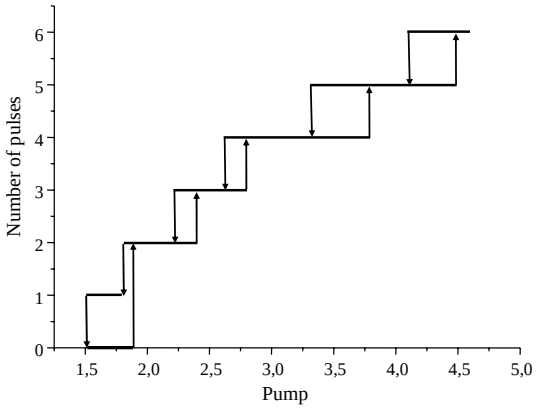


*Fig. 3. Experimental evolution of the number of pulses as a function of the pump power in the anomalous dispersion regime.*

The procedure to investigate the multiple pulsing is the following. The pump power is fixed to an intermediate value and then the different phase plates and polarization controllers are adjusted to obtain a regular signal consisting in several pulses by cavity round-trip. After

that, it is possible to measure the number of pulses for increasing and decreasing pumping power. We first consider the case of normal dispersion regime obtained with a total cavity length of about 22 m resulting in a repetition rate of 8.85 MHz. The average cavity second order group velocity dispersion (GVD) is $\beta_2 = 0.0026\,\mathrm{ps}^2/\mathrm{m}$. The experimental results are summarized in figure 2 which gives for a fixed pump power, the number of pulses coexisting in the laser cavity. When the pump power increases, the laser directly starts in the regime of 2 pulses by cavity round-trip. When the pumping is further increased, additional pulses appear one by one, up to 5. At this pumping level, if the power decreases, pulses disappear also one by one but for different values of switching powers. Results clearly demonstrate pump power hysteresis. Both the pump power evolution and the switching values depend on the exact adjustment of the phase plates. For example, the mode-locked regime can start with a single pulse when the pump is increased. Let us also mention that the switching powers are difficult to measure because even with a fast oscilloscope, pulses are not so easy to discriminate. In addition, environmental fluctuations lead to uncontrolled variation of the number of pulses. Similar results can be obtained in the anomalous dispersion regime. In the latter case, the total cavity length is about 18 m, corresponding to a repetition rate of about 10.78 MHz and the average GVD is $\beta_2 = -0.0017\,\mathrm{ps}^2/\mathrm{m}$. Experimental results are given in Fig. 3 and one can see that they are similar to those obtained in the regime of normal average dispersion.

### 3. Theory

In this section, we use a previously developed scalar theory to model the experimental results. We consider an erbium-doped fiber ring laser passively mode-locked through nonlinear polarization rotation. The setup is schematically represented in Fig. 4. For isotropic fibers this scheme involves all necessary elements for control of nonlinear losses. After the polarizing isolator the electric field has a well defined linear polarization. Such state of polarization does not experience polarization rotation in the fiber because the rotation angle is proportional to the area of the polarization ellipse [21]. Consequently, it is necessary to place a quarter wave plate 3 ($\alpha_3$ represents the orientation angle of one eigenaxis of the plate with respect to the laboratory frame). At the output of the fiber, the direction of the elliptical polarization of the central part of the pulse can be rotated towards the passing axis of the polarizer by the half wave plate 2 (the orientation angle is $\alpha_2$). Then this elliptical polarization can be transformed into a linear one by the quarter wave plate 1 (the orientation angle is $\alpha_1$). In this situation the losses for the central part of the pulse are minimum while the wings undergo strong losses. The setup of Fig. 4 has been modelled as follows [17]. The unique fiber has been assumed to have group velocity dispersion, optical Kerr nonlinearity and saturable gain. The nonlinear losses are described by solving in a first step the equations for a field propagating in a Kerr medium when dispersion is neglected, and then taking into account the three phase plates and the polarizer (self- and cross-phase modulation terms were considered together with four-wave mixing terms). On the other hand, a scalar equation has been written for a wave propagating in a saturable amplifying medium with GVD, to account for dispersion and gain. The resulting model assumes localized effect for the nonlinear loss due to the Kerr nonlinearity and the phase plates, while gain and GVD are distributed and averaged along the cavity. In dimensionless form, the final set of equations for the electric field amplitude is [17]

$$\frac{\partial E}{\partial \zeta} = \left(D_r + iD_i\right)\frac{\partial^2 E}{\partial \tau^2} + \left(G + i|E|^2\right)E, \quad (1)$$

$$E_{n+1}(\tau) = -\beta\begin{bmatrix}\cos(pI_n + \alpha)\cos(\alpha_1 - \alpha_3) + \\ + i\sin(pI_n + \alpha)\sin(\alpha_1 + \alpha_3)\end{bmatrix}E_n(\tau), \quad (2)$$

where $\zeta = z/L$, $\tau = t/\delta t$, $G = a\Big/\left(1 + b\int I d\tau\right)$, $D_r = GD_r^0 + d_r$, $D_r^0 = 2\Big/\left(|\beta_2|L\omega_g^2\right)$, $I_n = |E_n|^2$, $d_r = 2\rho_c/|\beta_2|$, $p = B\sin 2\alpha_3$, $a = g_0 L$, $b = I_r\delta t/\left(P_{sat}T_a\right)$, $\delta t = \sqrt{|\beta_2|L/2}$, $I_r = 1/\gamma L$, $\alpha = 2\alpha_2 - \alpha_1 - \alpha_3$.

$D_i$ and L (m) are the dispersion and the length of the fiber, respectively. $\gamma$ ($W^{-1}m^{-1}$) is the nonlinear coefficient related to the nonlinear index coefficient $n_2$, and $B = 1/3$ for silicate fibers [16]. $\beta$ is the transmission coefficient of the polarizer (free parameter). $\beta_2$ ($ps^2m^{-1}$) is the second order GVD. $T_a = Ln_0/c$ (s) is the photon round trip time, $n_0$ the linear refractive index, $c$ the velocity of light in free space, $g_0$ ($m^{-1}$) the unsaturated gain, and $P_{sat}$ (W) the saturating power.

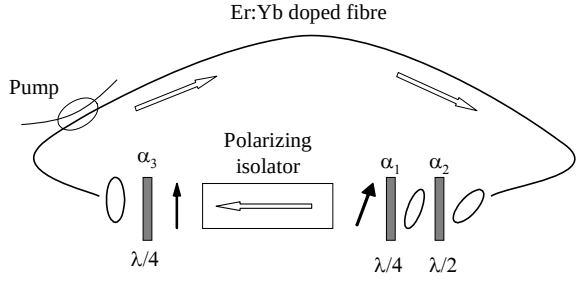


*Fig. 4. Schematic representation of a fiber ring laser passively mode-locked through non-linear polarization rotation.*

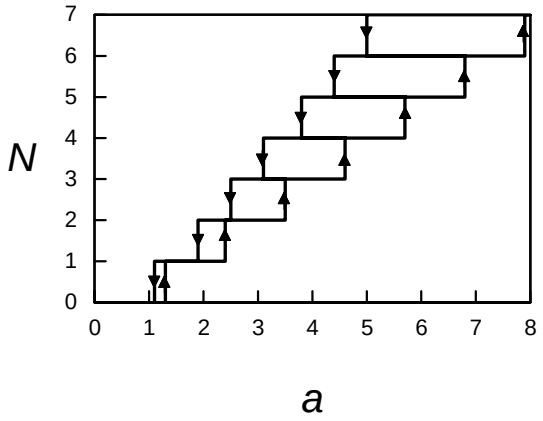


*Fig. 5. Hysteresis dependence of number of pulses in steady-state operation versus the pumping parameter a in the normal dispersion regime.*

$P_{sat} = \left(h\nu\pi r^2\right)/\left(\sigma T_1\right)$, where $h\nu$ (J) is the photon energy, $\sigma$ ($m^2$) the stimulated emission cross-section, $T_1$ (s) the lifetime of the upper level of the lasing transition, and $r$ (m) the radius of the fiber core, $\nu$ is the optical frequency and $h$ the Planck's constant. $\omega_g$ ($s^{-1}$) is the spectral gain bandwidth. $\rho_c$ describes the frequency-dependent loss due to both additional spectrally selective elements for control of a radiation spectrum or uncontrolled spectrally selective losses related with intracavity elements.

The numerical procedure starts from the evaluation of the electric field after passing through the Kerr medium, the phase plates and the polarizer, using equation (2). The resulting electric field is then used as the input field to solve equation (1) over a distance $L$, using a standard split-step Fourier algorithm. The computed output field is used as the new input for equation (2). This iterative procedure is repeated until a steady-state is achieved.

For the numerical simulations we use parameters adapted to silicate erbium-doped fibers: $\gamma = 3\times10^{-3}\,W^{-1}m^{-1}$, $c = 3\times10^{8}\,ms^{-1}$, $r = 5\times10^{-6}\,m$, $\sigma = 2.5\times10^{-24}\,m^2$, $T_1 = 8\times10^{-4}\,s$, $\omega_g = 10^{13}\,s^{-1}$ and $\beta = 0.95$. The fiber length L and the second order GVD $\beta_2$ will be adapted to the experimental conditions.

Multiple pulsing has been theoretically investigated in [17] and we report here the main results. Figure 5 shows an example of the evolution of the number of pulses $N$ versus the pumping parameter $a$. This result has been calculated in the normal dispersion regime for a particular position of the phase plates and for parameters corresponding to the experimental configuration ($L = 22\,m$, $\beta_2 = 0.0026\,ps^2/m$). For increasing pumping parameter, the laser is first continuous and then falls in the single-pulse mode-locked regime. If the pump is further increased, additional pulses appear one by one. If now the pump is decreased, the number of pulses disappears one by one for particular values of the pumping parameter $a$ but different from those obtained in the increasing way. Large pump power hysteresis domains are confirmed. Finally, additional numerical simulations show that the exact multistability and hysteresis sequence depend on the orientation of the phase plates. Hence, theoretical results favourably compare with experimental data in the normal dispersion regime. We have also tried to model the laser in the anomalous dispersion regime. Unfortunately, there is a systematic discrepancy between theory and experiment; therefore we do not report the theoretical result. This gives a limit of validity of the model which is based on an averaged approach over one cavity round-trip. As we have previously pointed out with a different model [16,22], an average treatment does not work correctly in the average negative dispersion regime [23]. It is expected that, in the anomalous dispersion case, a fully vectorial model, without any averaging along the cavity, could be more appropriate.

## 4. Conclusions

In summary, we have investigated both experimentally and theoretically the multiple pulsing

occurring in passively mode-locked fiber lasers. Mode-locking is obtained through nonlinear polarization rotation. Experimental study has been performed with an erbium-doped double-clad fiber laser with a management of the total cavity dispersion. The evolution of the number of pulses by cavity round-trip as a function of pump power exhibits pump power hysteresis and the pulses appear and disappear one by one. Experimental results are comparable in positive or negative GVD. Theoretical results favourably compare with experimental data in the normal dispersion regime while systematic differences exist in the anomalous case.

**Acknowledgements**

This research was supported by a Marie Curie International Fellowship within the 6th European Community Framework Programme.

## References

[1] A. G.Bulushev, E. M. Dianov, O. G. Okhotnikov, Opt. Lett. **16**, 88 (1991).
[2] D. J. Richardson, R. I. Laming, D. N. Payne, M. W. Phillips, V. J. Matsas, Electron. Lett. **27**, 730 (1991).
[3] M. Nakazawa, E. Yoshida, Y. Kimura, Appl. Phys. Lett. **59**, 2073 (1991).
[4] A. B. Grudinin, D. J. Richardson, D. N. Payne, Electron. Lett. **28**, 67 (1992).
[5] M. J. Guy, D. U. Noske, J. R. Taylor, Opt. Lett. **18**, 1447 (1993).
[6] V. J. Matsas, T. P. Newson, D. J. Richardson, D. N. Payne, Electron. Lett. **28**, 1391 (1992).
[7] K. Tamura, H. A. Haus, E. P. Ippen, Eletron. Lett. **28**, 2226 (1992).
[8] K. Tamura, E. P. Ippen, H. A. Haus, L. E. Nelson, Opt. Lett. **18**, 1080 (1993).
[9] D. Y.Tang, W. S. Man, H. Y. Tam, Opt. Com. **165**, 189 (1999).
[10] D. Y. Tang, W. S. Man, H. Y. Tam, P. D. Drummond, Phys. Rev. A **64**, 033814 (2001).
[11] P. Grelu, J. -M. Soto Crespo, J. Opt. B: Quantum Semiclass. Opt. **6**, 271 (2004).
[12] B. Ortaç, A. Hideur, T. Chartier, M. Brunel, P. Grelu, H. Leblond, F. Sanchez, IEEE Photon. Tech. Lett. **16**, 1274 (2004).
[13] H. A. Haus, J. G. Fujimoto, E. P. Ippen, IEEE J. Quant. Electron. **28**, 2086 (1992).
[14] L. E. Nelson, D. J. Jones, K. Tamura, H. A. Haus, E. P. Ippen, Appl. Phys. B **65**, 277 (1997).
[15] K. M. Spaulding, D. H. Yong, A. D. Kim, J. N. Kutz, J. Opt. Soc. Am. B **19**, 1045 (2002).
[16] H. Leblond, M. Salhi, A. Hideur, T. Chartier, M. Brunel, F. Sanchez, Phys. Rev. A **65**, 06381 (2002).
[17] A. Komarov, H. Leblond, F. Sanchez, Phys. Rev. A **71**, 053809 (2005).
[18] A. Komarov, H. Leblond, F. Sanchez, Phys. Rev. E **72**, 025604(R) (2005).
[19] M. Salhi, H. Leblond, F. Sanchez, Opt. Com. **247**, 181 (2005).
[20] A. Hideur, T. Chartier, M. Sahli, C. Özkul, M. Brunel, F. Sanchez, Opt. Com. **198**, 141 (2001).
[21] A. Haboucha, M. Salhi, A. Komarov, H. Leblond, F. Sanchez, J. Non. Opt. Phys. Mat. **15**, 157 (2006).
[22] M. Salhi, H. Leblond, F. Sanchez, Phys. Rev. A **67**, 013802 (2003).
[23] B. Ortaç, A. Hideur, M. Brunel, T. Chartier, M. Salhi, H. Leblond, F. Sanchez, Appl. Phys. B **77** 589 (2003).

*Corresponding author: francois.sanchez@univ-angers.fr